NJC

Accepted Manuscript

This is an *Accepted Manuscript*, which has been through the Royal Society of Chemistry peer review process and has been accepted for publication.

Accepted Manuscripts are published online shortly after acceptance, before technical editing, formatting and proof reading. Using this free service, authors can make their results available to the community, in citable form, before we publish the edited article. We will replace this *Accepted Manuscript* with the edited and formatted *Advance Article* as soon as it is available.

You can find more information about *Accepted Manuscripts* in the Information for Authors.

Please note that technical editing may introduce minor changes to the text and/or graphics, which may alter content. The journal's standard Terms & Conditions and the Ethical guidelines still apply. In no event shall the Royal Society of Chemistry be held responsible for any errors or omissions in this *Accepted Manuscript* or any consequences arising from the use of any information it contains.

ROYAL SOCIETY OF CHEMISTRY

www.rsc.org/njc

Cite this: DOI: 10.1039/c0xx00000x

www.rsc.org/xxxxxx

ARTICLE TYPE

Sol-Gel Process Activated by Visible Light-Emitting Diodes (LEDs) for Synthesis of Inorganic Films

Suqing Shi,[a,b] Xavier Allonas, [a] Céline Croutxé-Barghorn*[a] and Abraham Chemtob [a]

Received (in XXX, XXX) XthXXXXXXXXX 20XX, Accepted Xth XXXXXXXXX 20XX

DOI: 10.1039/b000000x

Photoinduced sol-gel polymerization is an efficient one-step and solvent-free process to synthesize inorganic or hybrid films. Highly condensed films are achieved by the use of photoacid generators (PAGs) generating *in situ* Brönsted superacids without thermal densification. However, most commercial PAGs exhibit short light absorption below 300 nm and display a limited overlap with the emission spectra of conventional UV sources, or with the newly emerging visible LED light sources. Therefore, the development of PAGs with extended absorption in UVA (λ> 380nm) is of paramount importance. In this study, a simple one-step visible LED induced sol-gel process of poly(dimethoxysiloxane) (PDMOS) was conducted by virtue of different photosensitized acid generating systems. The sol-gel process was followed by real-time Fourier transform infrared (RT-FTIR) spectroscopy. Hydrolysis rate and condensation of the siloxane network were directly correlated to the concentration of photogenerated acid. Different types of photosensitizers, onium cations and counter anions were investigated. Isopropylthioxanthone combined with iodonium salts bearing high charge delocalized anions led to the fastest and more efficient release of protonic acid, yielding tack-free and condensed transparent silica films.

1 Introduction

Recently, UV light induced sol-gel process has stood out as a fast one-step strategy to prepare a range of inorganic and nanocomposite films without the need for water and solvent.[1-4] In typical experiments, bulk films based on alkoxysilane precursors have been directly hydrolyzed and condensed through the catalytic action of Brönsted acids released upon UV-C (280-200 nm) and UV-B (280 – 315 nm) irradiation. Well-established onium salts photoacid generators (PAGs) have been employed - diaryliodonium ($Ph_2I^+X^-$) or triarylsulfonium ($Ph_3S^+X^-$) salts - similar as those widely reported in lithography and cationic photopolymerization.[5] For these original inorganic photopolymerizations, medium-pressure mercury lamps have been implemented leading to highly condensed silica-based films with rapid hydrolysis rates and minimal operational consumables.[2,4,6] Though mercury arc lamp technology is very efficient in this case, it is energy-intensive, requires frequent lamp replacement, and involves a toxic heavy metal, cooling system and high voltages.

Alternatively, visible light emitting diodes (LEDs) have attracted growing attention as emerging energy-efficient light sources for radiation curing with significant advantages, including safer emission wavelength, improved heat dissipation and life span, ozone-free and mercury-free environment-friendly technology as well as instant on/off controllability without lamp damage.[7-9] Because of its high peak irradiance and efficiency, the 395 nm LED has found in particular wide use in photopolymerization applications for electronics, composites, graphic arts.[9] However, most aforementioned PAGs only exhibit absorption bands confined to the short wavelength region of the UV spectrum (<300 nm), without overlapping with LED emission spectrum spanning 380-420 nm.[10] In order to match the spectral emission of visible LEDs, these photoinitiating systems need a modification. In cationic photopolymerization of epoxy or vinyl ether monomers, absorption shift towards visible range has been achieved thanks to additional long-wavelength photosensitizers (PSs) such as thioxanthone derivatives,[11-13] electron-rich polynuclear aromatic compounds[14-18] and curcumin[19]. These conventional PSs with different absorption and photophysical properties allowed the efficient PAG decomposition upon irradiation around their maximum absorption wavelength (λ_{max}). Their well-known mechanism proceeds by electron transfer photosensitization, as described in Scheme 1. PS is responsible for absorbing light energy and generating the excited species in the singlet or triplet state $^{1,3}PS^*$. The subsequent forward electron transfer from the excited $^{1,3}PS^*$ to the ground state of onium salt (On^+X^-) gives rise to a pair of PS radical cation ($PS^{+\bullet}$) and onium salt radical ($On^{\bullet}$).[10-19] In most cases, protonic acids (H^+X^-) recognized as the main initiating species are released by interaction of $PS^{+\bullet}$ with hydrogen donors (DH) or other photolytic radical species. [11-18] The yield and generation kinetics of photoacids are greatly affected by light absorption capability of the employed PS, deactivation of the excited $^{1,3}PS^*$ such as quantum yield of fluorescence (ϕ_f) and phosphorescene (ϕ_p),[10,11] driving force of electron transfer ($-\Delta G_{et}$)[11-18] and the

rate constants of forward and back electron transfer (BET),[12, 13,16,17] and so on.

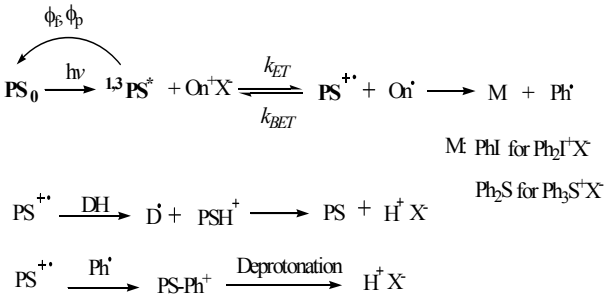

Scheme 1. Mechanism of photosensitized acid generation process

In the present paper, we demonstrate the first example of photosensitized sol-gel photopolymerization of trimethoxysilyl precursors films, opening the possibility of using a visible LED light source (λ = 395 nm) to produce inorganic silica films. Using diphenyliodonium hexafluorophospahte ($Ph_2I^+PF_6^-$) as PAG, the influence of five different PSs whose chemical structures are given in Table 1 has been thoroughly discussed as regards sol-gel process efficiency and photoacid generation rates. In addition, the effect of different PAG's cations and counter anions (Table 1) has been also studied using isopropylthioxanthone (**PS-I**) as PS. In all instances, no organic solvent is used and the various PAG/PS photoinitiating pairs have been directly dissolved in a poly(dimethoxysiloxane) (PDMOS) sol-gel precursor, a non-hydrolyzedoligomeric silicate derived from tetramethoxysilane.

2 Experimental

2.1 Materials

Anthracene (**PS-A1**, Fluka), 9,10-diethoxyanthracene (**PS-A2**, Acros Organics), 9,10-dimethylanthracene (**PS-A3**, Sigma-Aldrich), isopropylthioxanthone (**PS-I**, Fluka, a mixture of 2- and 4-isomers) and curcumin (**PS-C**, Sigma-Aldrich, recrystallized with 2-propanol before used) were used as PS. The employed onium salts were diphenyliodonium hexafluorophosphate (Iod-PF_6, Sigma-Aldrich), diphenyliodonium triflate (Iod-OSO_2CF_3, Sigma-Aldrich), diphenyliodonium *p*-toluenesulfonate (Iod-OSO_2PhCH_3, Sigma-Aldrich), diphenyliodonium chloride (Iod-Cl, Sigma-Aldrich), (4-methylphenyl)[4-(2-methylpropyl)phenyl]-iodonium hexafluorophosphate (Irgacure 250, supplied by BASF as 75% solution in propylene carbonate), (4-hydroxyethoxyphenyl)thianthrenium hexafluorophosphate (Esacure 1187, obtained from Lamberti as 75% solution in propylene carbonate) and bis(4-dodecylphenyl)iodonium hexafluorophosphate (UV 1242, Deuteron). Poly(dimethoxysiloxane) (PDMOS, ABCR) was used as inorganic precursor. Details concerning its structure were published elsewhere.[6] Quinaldine Red (QR, Sigma-Aldrich) was used as an acid sensor. All the products were used as received unless otherwise mentioned.

Table 1. Chemical structures of PSs, onium salts and methoxysilane oligomeric precursor PDMOS

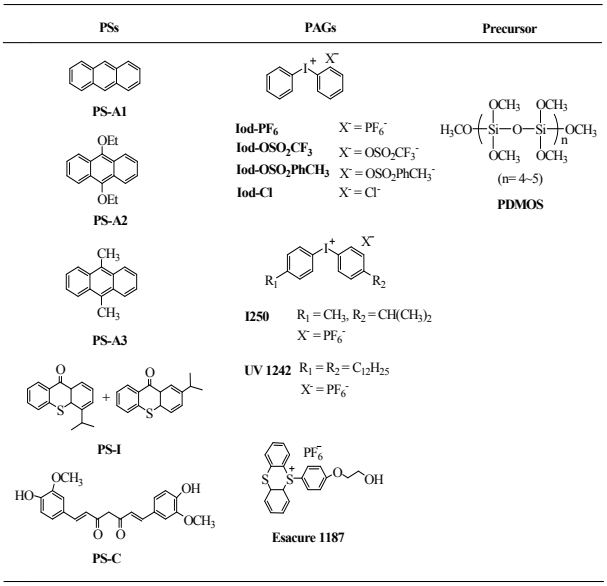

2.2 Photosensitized sol-gel polymerization of PDMOS

0.15 mol% of PAG, 0.40 mol% of PS and 30 wt% (based on PDMOS) of methanol/toluene (3/1, vol/vol) were added to PDMOS and stirred overnight in absence of light to obtain a homogeneous photosensitive formulation. Then, the obtained solution was spin-coated onto a BaF_2 pellet at 2000 rpm speed for 50 s (SPIN150, SPS) to produce a 0.9 ±0.2 μm liquid film layer. Visible light LED irradiation (irradiance = 20 $mWcm^{-2}$) was performed under air at room temperature by using a 395 nm LED device implemented on real time FTIR (Bruker Vertex 70, equipped with a liquid nitrogen cooled MTC detector, 4 cm^{-1} of resolution).[6] Upon irradiation, the evolution of various functional groups was simultaneously monitored by real-time FTIR. The hydrolysis of methoxysilyl (Si-OCH_3) group of PDMOS was followed at 2848 cm^{-1}. The formation of silanol (Si-OH) and hydroxyl (OH) group were followed at 930, and 3400 cm^{-1}, respectively. All spectra were baseline corrected prior to integration with the OPUS 6.5 software. All measurements were repeated at least three times and reproducible results were obtained. During the irradiation, the room humidity was maintained around 40~48% as checked with a hygrometer.

2.3 Acid generation rate

A solution of PS (0.06 mM) and onium salt (0.03 mM) containing ~ 10 ppm QR was prepared in acetonitrile. The initial QR absorbance (measured by Specord 210, Analytik Jena) of these solutions was ~1.0 at 520 nm (maximum absorption). The concentration of photogenerated Brönsted superacid was estimated by using a calibration curve of QR bleaching titrated with hexafluorophosphoric acid solution (HPF_6, 55 wt% in H_2O).[20]

3 Results and discussion

3.1 Spectroscopic and electrochemical properties of PSs

The light absorption and electrochemical properties of five conventional PSs, including anthracene derivatives (**PS-A1**, **PS-A2** and **PS-A3**), isopropylthioxanthone (**PS-I**) and curcumin (**PS-**

C), are summarized in Table 2. Their absorption spectra (see Figure S1 of Supporting Information) exhibit distinct overlapping behaviors with regard to the emission spectrum of the 395 nm LED, as exemplified by substantial differences of molar absorption coefficient at this given wavelength ($\varepsilon_{\lambda 395nm}$). Among the different PSs, **PS-I** has a maximum absorption (λ_{max}) at 384 nm leading to an acceptable $\varepsilon_{\lambda 395nm}$ value of 5160 M^{-1} cm^{-1}, while the three anthracene derivatives (**PS-A1-3)** possessing the typical absorption bands of polycyclic aromatic hydrocarbons reveal much lower $\varepsilon_{\lambda 395\ nm}$, especially for **PS-A1** (12 M^{-1} cm^{-1}). By contrast, **PS-C** strongly absorbs in the UV-Visible transition range (λ_{max} = 427 nm, $\varepsilon_{\lambda 395\ nm}$= 30300 $M^{-1}cm^{-1}$) due to the conjugation between the π-electron system of two feruloyl chromophores.[19] The free energy change of the photoreaction can be calculated from the Rehm Weller equation, taking into account that the coulombic interaction between the products is zero (equation 1).[14,18]

$$\Delta G_{et}\ (kJ/mol) = F\ [\ E_{ox}^{1/2} - E_{red}^{1/2}\ ] - E^{*} \qquad (1)$$

where F is the Faraday constant, $E_{ox}^{1/2}$ (V/SCE) the half-wave oxidation potential of PS, $E_{red}^{1/2}$ (V/SCE) the half-wave reduction potential of onium salt and E^{*} (kJ/mol) represents the excitation energy of the PS.

In all instances, the driving force for the photoinduced electron transfer ($-\Delta G_{et}$) is found to be greater than 90 $kJmol^{-1}$ (Table 1), showing that the aforementioned PSs are able to photosensitize the decomposition of iodonium salt PAGs via an electron transfer process, leading to the release of Brönsted acid.

Table 2. Spectroscopic and electrochemical properties of different PSs

	λ_{max} [nm]	$\varepsilon_{\lambda 395\ nm}$ [M^{-1} cm^{-1}]	[V/SCE]	E* [$kJmol^{-1}$]	ΔG_{et}[g] [$kJmol^{-1}$]
PS-A1	375, 355	12	1.16[a)]	316 ($^1E^*$)[a)]	-185
PS-A2	403, 381	2590	0.98[c)]	294 ($^1E^*$)[c)]	-180
PS-A3	397, 377	2161	0.87[b)]	309 ($^1E^*$)[b)]	-205
PS-C	427	30273	0.84[d)]	191 ($^3E^*$)[e)]	-91
PS-I	384	5161	1.5[f)]	256 ($^3E^*$)[f)]	-92

[a)](Ref [14]); [b)](Ref [18]);[c)](Ref [21],$E_{ox}^{1/2}$ and $^1E^*$ of **PS-A2** referenced as that of 9,10-dimethoxylanthracene); [d)](Ref [22]); [e)](Ref [23]); [f)](Ref [24]). [g)]ΔG_{et} is calculated by using $E_{red}^{1/2}$ of Iod-PF_6 as -0.2 V/SCE.[10b]

3.2 Effect of PS on the visible LED induced sol-gel process

FTIR spectroscopy is recognized as a powerful and simple technique to follow the evolution of silica sol-gel films and achieve a qualitative evaluation of the extent of the network condensation.[25] Real-time FTIR spectroscopy has recently emerged as a useful tool to investigate *in situ* the chemical and structural evolutions accompanying sol-gel polymerization of alkoxysilane films.[6,26-29] Of particular interest in our case is that the irradiation provided by a LED focused light (395 nm) can be synchronized with a rapid scan IR analysis (see experimental section). As a result, the progress of hydrolysis(equation 2) and condensation(equations 3-4) reactions within the PDMOS film can be monitored with a temporal resolution as low as 0.1 s. This characterization set-up has been helpful to assess the sol-gel photopolymerization efficiency of different PSs associated with the same PAG, $Ph_2I^+PF_6^-$ denoted as Iod-PF_6.

≡Si-OR + H_2O (atmospheric water) ↔ ≡Si-OH + ROH (2)

≡Si-OR + HO-Si≡ ↔ ≡Si-O-Si ≡ + ROH (3)

≡Si-OH + HO-Si≡↔≡Si-O-Si≡ + H_2O (4)

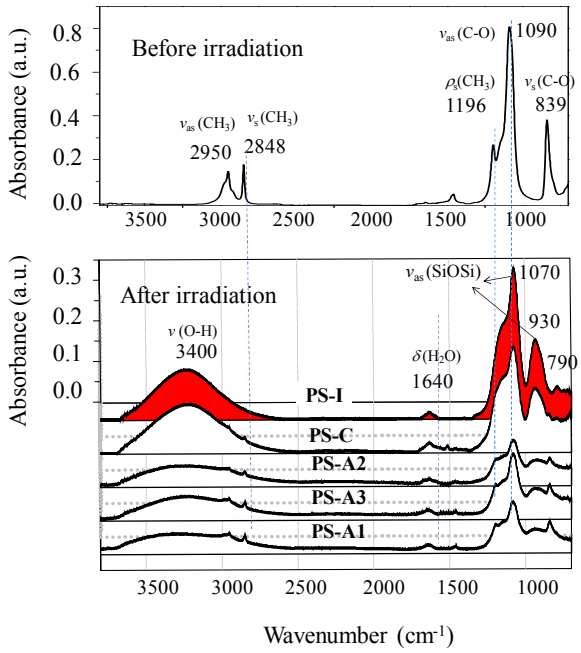

Fig. 1 FTIR spectra of PDMOS/Iod-PF_6 film before (top) and after sol-gel photopolymerization (bottom) in presence of different PSs mentioned directly on the spectra. The silica films were obtained after 100 s irradiation provided by a 395 nm LED. [PS]=0.4 mol%, [Iod-PF_6] = 0.15 mol%, irradiance = 20 mW cm^{-2}.

Hydrolysis proceeds by nucleophilic attack of water molecules onto the silicon center, and its kinetics strongly depends on the catalytic system.[27,30] Figure 1 shows the FTIR spectra of different silicate films (≈ 1µm) polymerized thanks to a series of PS/Iod-PF_6 during 100 s. Table 3 summarizes the major vibration bands of PDMOS present before and after irradiation, which are in agreement with IR data of the literature.[6,26,29] As shown in Figure 1, the PDMOS precursor spectrum exhibits (before reaction) the characteristic methoxysilyl ($SiOCH_3$) signals at 2950 and 2848 cm^{-1} corresponding to the neighboring out-of phase asymmetrical CH_3 stretching and asymmetrical CH_3 stretching. This well-resolved and sharp band can be used as marker of hydrolysis kinetics by monitoring its integrated absorbance over irradiation time. Additionally, other modes at 1196, 1090 and 839 cm^{-1} assigned respectively to CH_3 rocking, asymmetrical and symmetrical C-O stretching vibrations can be used to assess hydrolysis progress. In absence of PS, PDMOS does not undergo any hydrolysis reaction reflecting a total lack of absorption for the PAG used alone. Conversely, all the photosensitized PDMOS films demonstrate clear signs of hydrolysis as shown by a significant intensity decrease of the latter $SiOCH_3$ bands upon irradiation. As reported previously, the

photoacid-catalyzed hydrolysis of PDMOS films is presumably ensured by atmospheric moisture permeation within the film.[6] Figure 2A is a plot of hydrolysis degree (D_h) as a function of irradiation time for different PSs investigated. For the three anthracene-based PS, hydrolysis is limited to ca. 90%, whereas **PS-C**and **PS-I** yield a complete hydrolysis. The **PS-I**/Iod-PF_6 system exhibits the fastest hydrolysis rate with full conversion achieved in only 37 s. In this case, the disappearance of the Si-OCH_3 moieties coincides entirely with the growth of two IR bands indicative of Si-OH groups such as the Si-O (930 cm^{-1}) and O-H (3400 cm^{-1}) stretching vibrations (Figure 2B).[6]

Table 3. Main absorption bands of PDMOS before and after 395 nm LED induced sol-gel process

Wavenumber (cm^{-1})	Before irradiation IR modes	Wavenumber (cm^{-1})	After irradiation IR modes
2950	$\nu_{as}(CH_3)$	~3400	ν (OH) (hydrogen bonded)
2848	$\nu_s(CH_3)$	~1640	δ (H_2O) (bending)
1196	$\rho(CH_3)$	~1070-1080	ν_{as}(Si-O-Si)
1090	ν_{as}(C-O)	~1030	ν_{as}(Si-O-Si)
839	ν_s(C-O)	930	ν (Si-O^-), ν (Si-OH)
		790	ν_s(Si-O-Si)

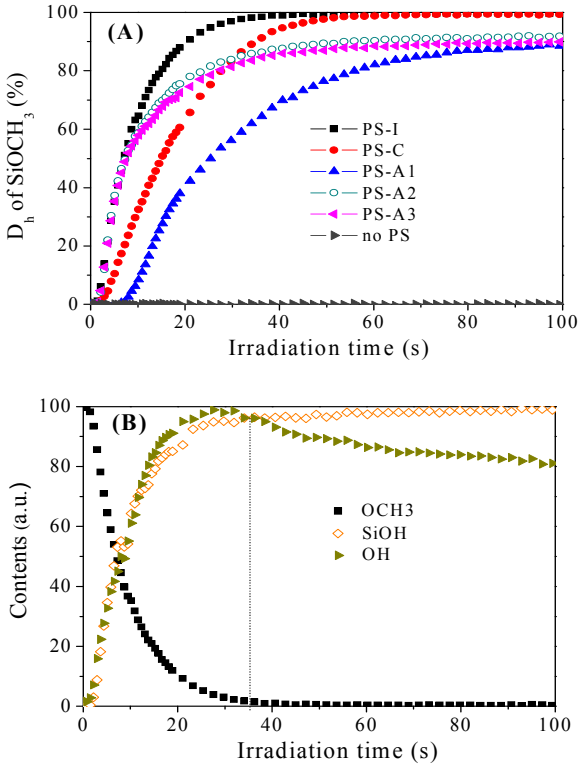

Fig. 2(**A**) Hydrolysis degree (D_h, %) of $SiOCH_3$ in PDMOS photocatalyzed by different PS/Iod-PF_6 systems. (**B**) Area evolution (integrated absorbance) of $SiOCH_3$ (2848 cm^{-1}), OH (~3400 cm^{-1}) and SiOH (930 cm^{-1}) bands during the irradiation of PDMOS/**PS-I**/Iod-PF_6 film. [PS] = 0.4 mol%, [Iod-PF_6] = 0.15 mol%, irradiance = 20 mW cm^{-2}.

Condensation starts as early as Si-OH groups (930 cm^{-1}) are generated by hydrolysis, to yield linear, branched or cyclic siloxane structures. [6,25,26,30] This reaction concomitant to hydrolysis can be firstly evidenced in Fig. 2B by the marked decrease in the area of the OH band at 3400 cm^{-1} after 35 s irradiation. This band corresponds to the different hydroxyl containing species (silanol groups, methanol and water that are the by products of the sol-gel reaction). Therefore, its decrease mainly results from condensation reactions and evaporation of methanol as already reported. [6] Condensation is also clearly noticeable in Fig. 1 from the presence of the typical Si-O-Si asymmetric stretching (ν_{as}(Si-O-Si)) band[25-29] in the 1000-1300 cm^{-1} range. In the literature, this broad absorption band has been assigned to an overlap of two pairs of transverse optical (TO) and longitudinal optical (LO) modes. By using a conventional curve fitting, this latter has been successfully resolved into four Lorentzian peaks: ~1070-1080 cm^{-1} (TO_3), ~1200 cm^{-1} (LO_3), ~1157-1170 cm^{-1} (TO_4) and ~1130 cm^{-1} (LO_4). Fig.3A gives the deconvolution results for the PDMOS/**PS-I**/Iod-PF_6, but similar results have been obtained for the other PSs (see Fig.S2 of Supporting Information). Among these different peaks, the most intense at ~1070-1080 cm^{-1} (TO_3) has been used as a marker to probe qualitatively the photoinduced condensation reaction.[25,30] In several studies, the increase of the TO_3 band has been correlated with more pronounced condensation of the silanol groups.[28] Fig.3B shows on the same plot the aspect of the TO_3 peak for the five different PSs implemented in this study. As expected from the first part, **PS-I** results in the most intense TO_3 peak, indicating presumably a more efficient condensation process compared with the other photoacid generating systems. In this case, there is additionally a significant upward shift of the TO_3 position during irradiation, from 1065 cm^{-1} to 1070 cm^{-1}, suggestiveof a densification of the silica network (Fig.S3, Supporting Information). This result is in good agreement with the production of tack-free solid film after an illumination of 100 s. By contrast, the slight downshift of TO_3 peak for the other PSs may reveal porosity and a reduced density (Fig.S3, Supporting Information).[26,29,30]

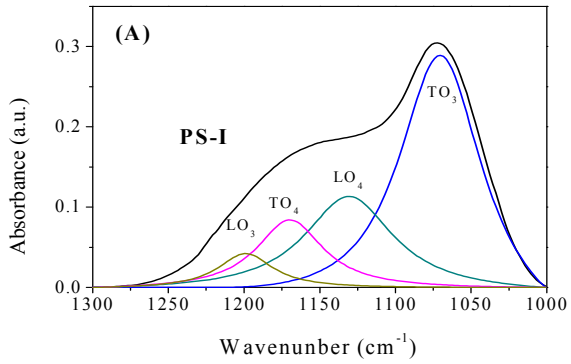

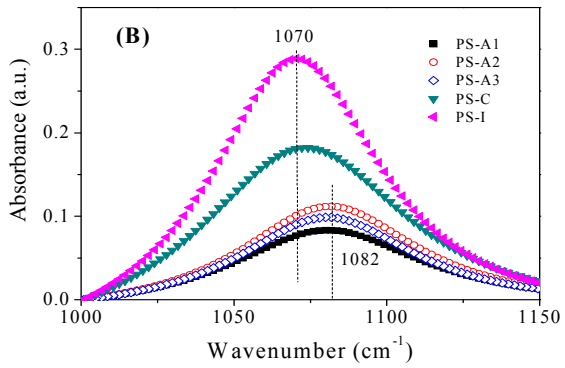

Fig. 3(A) Deconvolution of the Si-O-Si stretching band of the polymerized PDMOS film photocatalyzed by **PS-I**/Iod-PF_6, (B) The effect of PSs on the evolution of TO_3 mode vibration. [PS] = 0.4 mol%, [Iod-PF_6] = 0.15 mol%, irradiance = 20 mW cm^{-2}, irradiation time = 100 s.

The type of PS greatly influences hydrolysis and condensation kinetics of PDMOS/Iod-PF_6 film under 395nm-LED irradiation. We postulate that the formation rate of $H^+PF_6^-$ superacids and its final concentration are the major parameters controlling the sol-gel process efficiency. Whether this assumption is valid can be assessed by a colorimetric acid/base titration during 395 nm LED irradiation using QR as acid marker. The decrease of its maximum absorption at 520 nm (basic form), in a region sufficiently distinct from the PS absorption range, serves to monitor the extent of photoacids generated upon UV irradiation.[20]

As seen in Fig.4, the three anthracene derivatives (**PS-A1-3**) that are typical singlet sensitizers of onium salts generate a very low amount of $H^+PF_6^-$ upon 395 nm LED irradiation despite their high electron transfer driving force ($-\Delta G_{et}$ = 180 ~ 205 kJ/mol). This result can be interpreted in the light of their low absorption ability, high ϕ_f in non-protonic solvent (0.27, 0.68 and 0.9 in acetonitrile for **PS-A1**, **PS-A2** and **PS-A3**, respectively)[17, 32] and fast back electron transfer (BET) rate constant (5×10^{10} and $<3\times10^{10}$ s^{-1} for **PS-A1**$^{+\bullet}$ and **PS-A2**$^{+\bullet}$, respectively).[16,17] A slow and limited acid photogeneration is fully consistent with the partial hydrolysis of the $SiOCH_3$ functions and the limited Si-O-Si network detected by RT-FTIR. In contrast, the well-known triplet sensitizer **PS-I** promoted the very efficient decomposition of Iod-PF_6, thus releasing a much higher concentration of $H^+PF_6^-$ at faster rate, which is in agreement with the previous FTIR data. This result may be explained by the synergistic effect of an acceptable light harvesting capability, low deactivation behavior in acetonitrile (ϕ_f =0.005), [33] high quantum yield of triplet formation (ϕ_T) (0.66)[33] and efficient interaction rate constant between ^{3}PS-I and diphenyliodonium salt with rate constant of $>10^9$ s^{-1}.[12,34] Unfortunately, measuring acid generationfor thePS-C/Iod-PF_6 system has not been possible because of the basic properties of curcumin interfering with QR. A protonated curcumin was formed within a few tens of picoseconds in weak acidic solution, generating a new band well-overlapped with the QR absorption at 520 nm.[35,36] Obviously, deactivation reaction of photoacids with curcumin may compete with the catalysis of sol-gel process, thus reducing the catalytic reactivity and contributing to a lower hydrolysis rate than that of **PS-I**/Iod-PF_6.

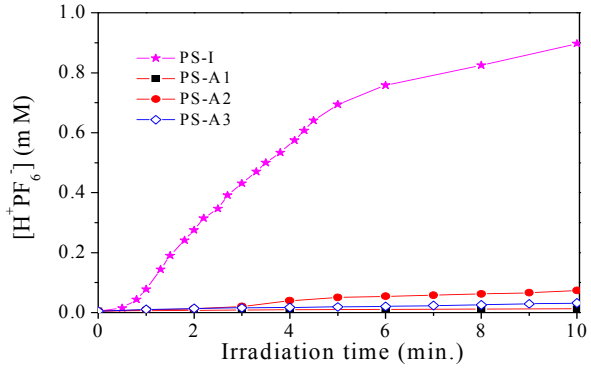

Fig.4 The effect of PS on the generation of $H^+PF_6^-$. Measurements were performedin acetonitrile. [PS] = 0.06 mM, [Iod-PF_6] = 0.03 mM, irradiance = 40 mW cm^{-2}.

3.3 Influence of the PAG structure in a photosensitized sol-gel process

Fig.5 compares the hydrolysis efficiency of different PAGs associated with the most efficient sensitizer **PS-I**. Both the oxidation ability of the cation, and the size/nucleophilicity of the counter anions are known to affect hydrolysis. As shown in Fig.5A, the diphenyliodonium salts with a higher charge delocalized anion, including Iod-PF_6 and Iod-OSO_2CF_3, lead to a fast (the rate of hydrolysis is 6.56-10.0 s^{-1}) and complete hydrolysis. In contrast, *p*-toluenesulfonate anion yielding the weaker *p*-toluenesulfonic acid results in slower and partial hydrolysis and therefore tacky and even liquid surface. In addition, Fig.5B reveals a much higher reactivity of the iodonium salts compared to sulfonium salts, keeping the same counter-anion (PF_6^-). We think that $SiOCH_3$ hydrolysis is predominantly governed by the oxidation ability of the onium cation. The higher reduction potential of the iodonium cation (-0.2 V/SCE for diphenyliodonium) [10b,34] drives a much higher hydrolysis rate, compared to the sulfonium cation (Esacure 1187).[37]

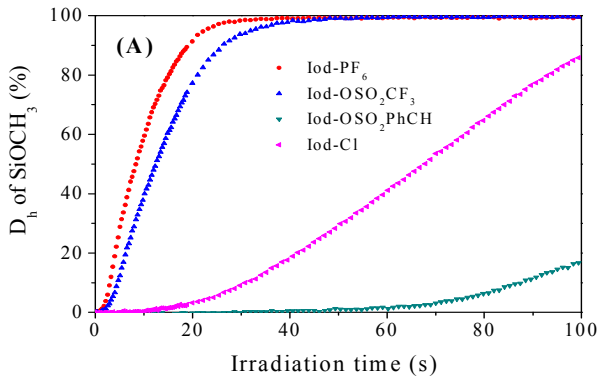

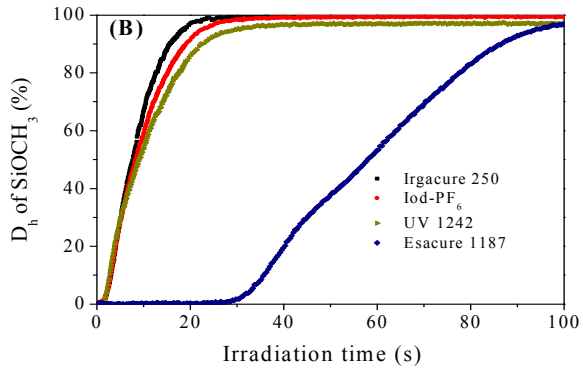

Fig. 5 D_h of $SiOCH_3$ in PDMOS photocatalyzed by different **PS-I**/PAG systems upon 100 s of irradiation at 395 nm. (A) Effect of counter anions of diphenyliodonium salts and (B) the effect of cation structure of onium hexafluorophosphates. [PS-I] = 0.4 mol%, [Iod-PF_6] = 0.15 mol%, irradiance = 20 mW cm^{-2}.

The acid strength of the photogenerated acid (HX) relies on the H-X bond dissociation ability and the nucleophilicity of counter anions.[20] As expected, the order of acid generation rate for the various **PS-I**/diphenyliodonium salts pairs follows the order Iod-PF_6 > Iod-OSO_2CF_3 > Iod-OSO_2PhCH_3 > Iod-Cl keeping the same diphenyliodonium cation unchanged (Fig.6A). With the same PF_6^- counter anion, the reactivity order is Irgacure 250 > Iod-PF_6> UV 1242 > Esacure 1187 (Fig.6B). These results are in agreement with a previous study on photosol-gel reaction under UV light. [6,31] It was thus reasonable to conclude that in the presence of **PS-I** as sensitizer, the higher catalytic reactivity for the sol-gel process was correlated to a higher degree of oxidation ability of the onium cation, a greater distance between the cation and counter anion, a weaker coordination of the anion and a stronger protonic acid generated.

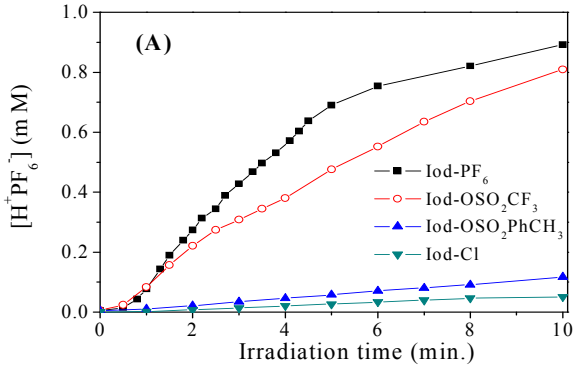

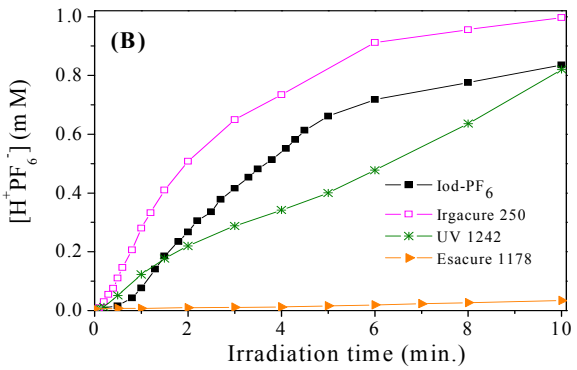

Fig. 6 The effect of onium salts on protonic acid generation behavior in acetonitrile. (A) Effect of the counter anions in diphenyliodonium salts, and (B) effect of cation structure of onium salt based on hexafluorophosphate. [PS-I] = 0.06 mM, [onium salt] = 0.03 mM, irradiance = 40 mW/cm^2

3.4. Proposed mechanism of acid generation

PS-I/iodonium salt systems with highly delocalized counter anions can photoinduce very efficiently the sol-gel process under visible light LED irradiation. This result could be explained by the very rapid and high concentration of released acid. As shown in the photobleaching experiments of PS-I/Iod-PF_6 in acetronitrile solution in presence of QR as acid sensor, the rapid release of protonic acid was only accompanied by a very slight decrease of PS-I absorption (Fig.S4, Supporting Information), suggesting the simultaneous regeneration of PS-I during the irradiation. We speculate that two mechanisms involved both in the acid release and regeneration of PS-I may contribute to the high sol-gel reactivity: first, the electron transfer photosensitization process (Scheme 2, path a) between the triplet PS-I and ground state of iodonium salt [11,33]; second, the hydrogen abstraction from possible hydrogen donors (DH), i.e. methoxysilyl moieties in PDMOS or the *in situ* generated methanol byproduct, yielding PS-IH• radical species (Scheme 2, path b). In the latter pathway, the resulting PS-IH• can be easily oxidized by Iod-PF_6, releasing protonic acid through regenerating PS-I. [38] Both pathways may account for the highly efficient acid generation behavior and the resulting high catalytic reactivity of the sol-gel process under LED irradiation

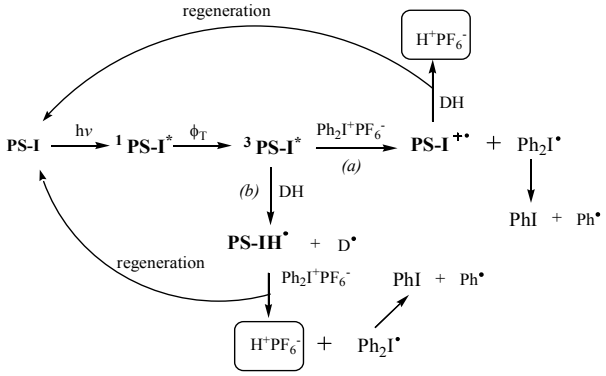

Scheme 2. The assumed mechanism for the efficient acid generation behavior of PS-I/Iod-PF_6

4 Conclusion

Photoacid catalyzed sol-gel polymerization was performed for the first time under 395 nm visible light-emitting diode irradiation using various photoacid generating systems. A combination of RT-FTIR spectroscopy and acid generation measurement provided a clear picture of hydrolysis and condensation reactions yielding transparent solid silica film. The spectral absorption and physical properties of the photosensitizers, oxidation ability of onium salts were the major features of governing the effectiveness of this photosensitized inorganic photopolymerization. Photosensitizers exhibiting acceptable light absorption ability at 395 nm, high reduction capability and quantum yield of the effective excited state led to a rapid liberation of photoacid. Onium salts with high reduction potential and delocalized and non-nucleophilic counter anion resulted in higher driving force for the electron transfer process and generated strong protonic acids. The couple isopropylthioxanthone and diphenyliodonium hexafluorophosphate was the most efficient photoinitiating system. We believe that these results could pave the way for a more sustainable approach towards inorganic or hybrid materials under solar or visible light.

Acknowledgement

The authors would like to thank Shaanxi Province Youth Science & Technology Star Projects (No.2014KJXX-62), China Scholarship Councial (CSC), Académie des Sciences Fondation Franco-Chinoise pour la Science et ses Applications (FFCSA) and ANR DeepCure project (#ANR-13-CHIN-0004-01) for their financial supports.

Notes and References

[a]*Laboratory of Macromolecular Photochemistry and Engineering, University of Haute-Alsace, ENSCMu, 3 rue Alfred Werner, 68093 Mulhouse Cedex, France.Fax: +33(0)389335014; Tel: +33(0)389335017; Email: celine.croutxe-barghorn@uha.fr (C. Croutxe-barghorn)*

[b]*Key Laboratory of Synthetic and Natural Functional Molecule Chemistry of Ministry ofEducation and College of Chemistry & Material Science, Northwest University, Xuefu Ave.,Guodu, Chang'an District, Xi'an 710127, PR. China. Fax: +86(0) 29 81535026;Tel: +86 29 81535032;Email: shisq@nwu.edu.cn (S. Shi)*

† Electronic Supplementary Information (ESI) available: [UV-Vis spectra of all the PSs and the emission spectrum of 395 nm LED, deconvolution of Si-O-Si stretching band of cured PDMOS films photocatalyzed by PS/Iod-PF_6, evolution of ν_{as}(Si-O-Si) vibrationalfrequencies, UV spectra changes of PS-I/Iod-PF_6 on irradiation of 395 nm LED under air in acetonitrile]. See DOI: 10.1039/b000000x/

1 Y. Wei, W. Wang, J. M. Yeh, B. Wang, D. Yang and J. K. Murray, *Adv. Mater.,*1994, **6**, 372.

2 (a) A. Chemtob, D. L. Versace, C. Belon, C. Croutxé-Barghorn and S. Rigolet, *Macromolecules,* 2008, **41**, 7390; (b) C. Belon, A. Chemtob, C. Croutxé-Barghorn, S. Rigolet, V. Le Houérou and C. Gauthier, *J. Polym. Sci. Part A: Polym. Chem.,*2010, **48**,4150.

3 X. Sallenave, O. J. Dautel, G. Wantz, P. Valvin, J. P. Lère-Porte and J. J. E. Moreau, *Adv. Funct. Mater.,*2009, **19**, 404.

4 (a) L. Ni, A.Chemtob, C. Croutxé-Barghorn, N. Moreau, T. Bouder, S. Chanfreau and N. Pébère, *Corrosion Science,*2014, **89***,* 242; (b) L. Ni, S. Rigolet, A. Chemtob and C. Croutxé-Barghorn, J. Brendlé, L. Vidal, *C. R. Chimie,* 2013, **16**, 897.

5 (a) J. V. Crivello and S. K. M. Jang, *Macromol. Symp.* 2004, **217**, 47; (b) M. Sangermano, *Pure Appl.Chem.,* 2012, **84**, 2089.

6 H. De Paz, A. Chemtob, C. Croutxé-Barghorn, D. Le Nouen and S. Rigolet, *J. Phys. Chem., B*2012, **116**, 5260.

7 F. Courtecuisse, J. Cerezo, C. Croutxé-Barghorn, C. Dietlin and X. Allonas, *J. Polym. Sci. Part A: PolymChem.,* 2013, **51***,* 635.

8. N. S. Kenning, B. A. Ficek, C. C. Hoppe and A. A. Scranton, *Polym. Inter.,* 2008, **57***,* 1134.

9 K. C. Anyaogu, A. A. Ermoshkin, D. C. Neckers, A. Mejiritski, O. Grinevich and A.V. Fedorov, *J. Appl. Polym. Sci.,*2007, **105,** 803.

10 (a) J. V. Crivello, *Adv. Polym. Sci.,*1984, **62**, 1; (b) Y. Yagci and I. Reetz, *Prog. Polym. Sci.,*1998, **23**, 1485.

11 P. E. Sundell, S. Jönsson and A. Hult, *Polym. Sci. Part A: Polym. Chem.,*1991, **29,** 1525.

12 G. Maniannan and J. P. Fouassier, *J. Polym. Sci. Part A: Polym. Chem.,*1991, **29,** 1113.

13 R. Rodrigues and M. G. Newmann, *Macromol. Chem. Phys.,* 2001, **202,** 2776.

14 Y. Toba, *J. Polym. Sci. Part A: Polym. Chem.,*2000, **38,** 982.

15 J. V. Crivello and M. Jang, *Photochem. Photobiol. A: Chem.,* 2003, **159,** 173.

16 R. J. Devoe, M. R. V. Sahyun, E. Schmidt, N. Serpone and D. K. Sharma, *Can. J. Chem.,*1988, **66,** 319.

17 R. J. Devoe, M. R. V. Sahyun, E. Schmidt and D. K.Sharma, *Can. J. Chem.,*1990, **68,** 612.

18 E. Gerd and N. Goez, *J. Am.Chem.Soc.,*1999, **121,** 2274.

19 (a) J. V. Crivello and U.Bulut, *Macromol. Symp.,* 2006, **202,** 1; (b) J. V. Crivello and U.Bulut, *J. Polym. Sci. Part A: Chem.,*2005, **43,** 5217.

20 K. Ren, J. H. Malpert, H. Li, H. Gu and D. C. Neckers, *Macromolecules,*2002, **35,** 1632.

21 E. Hasegawa, S.Takizawa, T. Seida, A. Yamaguchi, N. Yamaguchi, N. Chiba, T. Takahashi, H. Ikeda and K. Akiyama, *Tetrahedron,*2006, **62,** 6581.

22 K. I. Priyadarsini, D. K. Maity, G. H. Naik, M. S. Kumar, M. K. Unnikrishnan, J. G. Satav and H. Mohan, *Free Radical Biology & Medicine,* 2003, **55,** 475.

23 A. A. Gorman, I. Hamblett, V. S. Srinivasan and P. D. Wood, *Photochem. Photobiol.,*1994,**59,** 389.

24 J. P. Fouassier, X. Allonas, J. Lalevee and M. Visconti, *J. Polym. Sci. A: Polym. Chem.,*2000, **38**, 4531.

25 P. Innocenzi, *J. Non-Cryst. Solids*, 2003, **316**, 309-319.

26 J. Y. Chen, F. M. Pan, A. T. Chao, K. J. Chao,T. G. Tsai, B. W. Wu, C. M. Yang and L. Chang, *J. Eletrochem. Soc.,*2003, **150,** F123.

27 A.Vincent, S. Badu, E. Brinley, A.Karakoti, S. Deshpande and S.Seal, *J. Phys.Chem.,C* 2007, **111**, 8291.

28 A. A. Letailleur, F. Ribot, C. Boissière, J. Teisseire, E. Barthel, B. Desmazières, N. Cheminand C. Sanchez, *Chem. Mater.,* 2011, **23**, 5082.

29 L. Toniutti, S. Mariazzi, N. Patel, R. Checchetto, A. Miotello and R.S. Brusa, *Appl. Surf. Sci.,*2008, **255**, 170.

30 A. D. Chomel, P. Dempsey, J. Latournerie, D. Hourlier-Bahloul and U. A. Jayasooriya, *J. Chem. Mater.,*2005, **17**, 4468.

31 A. Kowalewska, *J. Mater. Chem.*2005, **15**, 4997.

32 S. Samori, S. Tojo, M. Fujitsuka and T. Majima, *Photochem.Photobiol.,*2009, **205**,179.

33 H.-J. Timpe, K.-P. Kronfeld and U. Lammel, *J. Photochem. Photobio. A: Chem.,*1990, **52**, 111.

34 J. Lalevee, M. El-Roz, X. Allonas and J. P. Fouassier, *J. Polym. Sci. A: Polym. Chem.,* 2008, **46**, 2008.

35 K. Akulov, R. Simkovitch, Y. Erez, R. Gepshtein, T. Schwartz and D. Huppert, *J. Phys.Chem A.,*2014, **118**, 2470.

36 Y. Erez, R. Simkovitch, S. Shomer, R. Gepshtein and D. Huppert, *J. Phys. Chem A.,*2014, **118**, 872.

37 S. Telitel, F. Dumur, T. Faury, B. Graff, M. A. Tehfe, D. Gigmes, J. P. Fouassier and J. Lalevée, *Beilstein J. Org.Chem.,*2013, **9**, 877.

38 D. Dossow, Q. Q. Zhu, G. Hizal, Y. Yagci and W. Schnabel, *Polymer,*1996, **37**, 2821.

TEXT:

Photosensitized sol-gel photopolymerization of trimethoxysilyl precursors films opens the possibility of using a visible LED light source (λ = 395 nm) for inorganic photopolymerization. It also provides a simple approach for sustainable synthesis of inorganic or hybrid materials under solar irradiance.

Graphic: